# Estimation of Dissolved Structures of Mono- and Dinuclear Chromate Species in Solution Using UV-vis Absorption Spectra and Molecular Orbital Calculation DV-Xα

Toru OZEKI,* Yoshihiro KINOSHITA, Hirohiko ADACHI,† and Shigero IKEDA††
Hyogo University of Teacher Education, Shimokume, Yashiro, Kato, Hyogo 673-14
† Faculty of Technology, Kyoto University, Yoshida-honmachi, Sakyo-ku, Kyoto 606
†† Department of Material Chemistry, Faculty of Science and Technology, Ryukoku University, Seta, Otsu 520-21

(Received November 29, 1993)

The dissolved structures of mono- and dinuclear chromate species, $CrO_4^{2-}$, $HCrO_4^-$, $H_2CrO_4$, and $Cr_2O_7^{2-}$ in aqueous solution were estimated by optimizing their structure models so that UV-vis absorption spectra reproduced from molecular orbital calculation DV-Xα fitted to the experimentally obtained component spectra. It is demonstrated that bond order obtained by Mulliken's population analysis gives useful information to explain why dimerization reaction of $HCrO_4^-$ to form $Cr_2O_7^{2-}$ proceeds easily.

Chromate salts are useful oxidizing agents due to its strong oxidation ability; but the reactivity depends upon the pH of the solution. There are a variety of chromium(VI) species in solution. In neutral or alkaline solutions, chromium(VI) exists as a tetrahedral inert ion $CrO_4^{2-}$.[1] In acid solution, protonation gives rise to a hydrogen chromate ion ($HCrO_4^-$)[2] and a dihydrogen chromate (chromic acid, $H_2CrO_4$).[3] Dichromate ion, $Cr_2O_7^{2-}$, is also formed in the high concentration solution ($>10^{-4}$ mol dm$^{-3}$) of $HCrO_4^-$ in the pH range 1—5. The hydrogen dichromate ion, $HCr_2O_7^-$, was once reported,[3] but later was found to be insignificant in most studies.[4,5]

The hydrogen chromate ion $HCrO_4^-$ has a tendency to easily form esters with other species containing –OH groups. The formation of the dichromate ion is the archetype of this reaction.

$$2HCrO_4^- \rightleftharpoons Cr_2O_7^{2-} + H_2O \quad (1)$$

Changes in the electronic absorption spectra of $HCrO_4^-$ in the presence of oxyacids, such as $HSO_4^-$, $H_2PO_4^-$, $HPO_3^-$, and $HS_2O_3^-$, have been interpreted as indicating formation of the 1 : 1 esters.[1] Kinetics of the oxidation of the solution indicates that the formation of such esters precedes the redox processes. The $HCrO_4^-$ exchanges rapidly the oxygen with solvent water although the $CrO_4^{2-}$ is relatively inert.[6] For most redox reaction the equilibrium described by Eq. 1 is established more rapidly than the redox reaction proceeds; and it is impossible to determine whether the rate law depends on $[HCrO_4^-]^2$ or $[Cr_2O_7^{2-}]$, although the latter interpretation is favored.[1] Equilibrium constants on chromium(VI) ions have been reported elsewhere.[7—10]

An analogous oxyacid molybdate rather prefers much aggregated species such as heptamer or octamer.[11,12] In order to understand the difference of the reactivity on aggregation, the details on the electronic states of the monomer species in solution have to be known. If the informations on the dissolved structures of these species are given, their electronic states are also obtained through the molecular orbital calculation (MO).

The conventionally available methods to determine the dissolved structure of the species in solution, X-ray diffraction, neutron diffraction, EXAFS, and so on, are however not adequate for this sort of solution system containing very low concentration species such as the $HCrO_4^-$. On the other hand, ultraviolet/visible (UV-vis) absorption spectra come from electronic transitions between molecular orbital levels of the species. If the structure of the ion changes, the UV-vis spectrum also changes. It is possible to optimize the structure model of the species so that the spectrum expected from the MO calculation using the structure fits to the measured spectrum.[13]

Usually the UV-vis spectrum measured by the experiment is overlapped one to which a couple of species contribute. In such cases a chemometrical technique, a factor analysis with equilibrium constraints (FAEC),[12] can be applied to extract pure component spectrum for each component species.

In this study, several possible structures of chromium (VI) ions were assumed as shown in Fig. 1; and the most probable structures of the species in solution were estimated. In addition, the relationship between the electronic states and reactivity on dimerization was examined. The effect of hydration of the $CrO_4^{2-}$ ion on its UV-vis spectrum was also discussed.

## Experimental

UV-vis absorption spectra of the solutions of $6\times10^{-4}$ mol dm$^{-3}$ $Na_2CrO_4$ and 0.5 mol dm$^{-3}$ $NaClO_4$ with various pH values (from −1.5 to 9) adjusted with NaOH or $HClO_4$ were obtained. In the case that the concentration of used $HClO_4$ was higher than 0.5 mol dm$^{-3}$, the value of pH was calculated from the activity: the product of nominal concentration of $HClO_4$ and activity coefficient.[14] The UV-vis spectra of the solutions of various concentrations (from $6\times10^{-4}$ to $5\times10^{-3}$ mol dm$^{-3}$) of $Na_2CrO_4$ with pH 3.5 were also measured. The FAEC was applied to these spectra; and

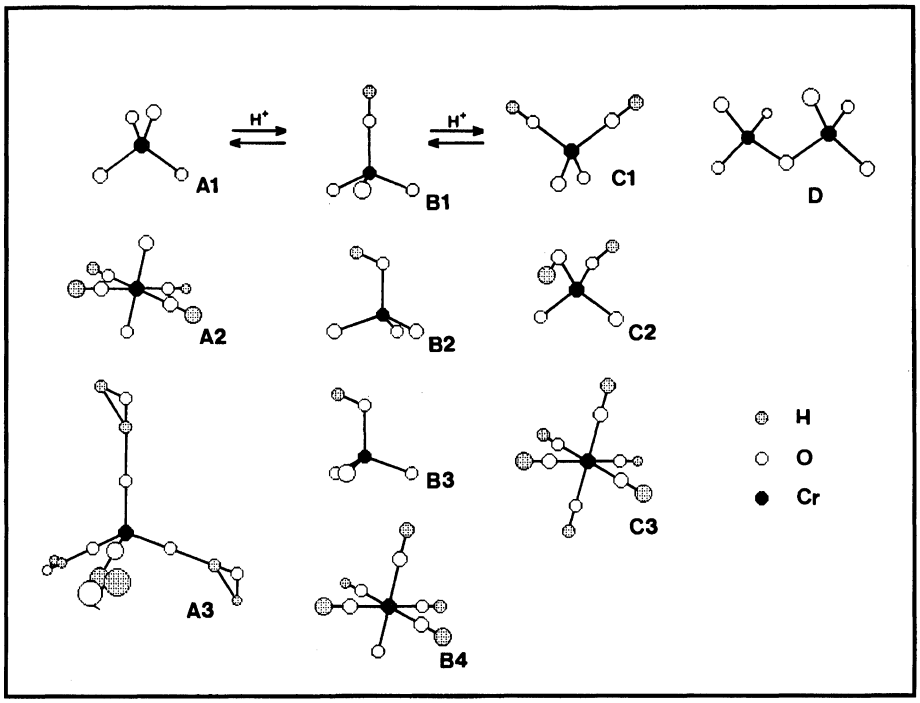


Fig. 1. Illustrations of cluster models used for the molecular orbital calculations. As to the values of bond length and bond angle, see Table 1.

the pure component spectra of $CrO_4^{2-}$, $HCrO_4^-$, $H_2CrO_4$, and $Cr_2O_7^{2-}$ were extracted. These spectra are consistent with the ones already reported elsewhere.[1] In the following, the term 'observed spectrum' is used to remark the pure component spectrum extracted by the FAEC.

In order to get the correct peak positions of a spectrum, peak separation treatment was carried out for each observed spectrum, after the abscissa was altered from nm-unit into eV-unit. Here, a peak was modeled by a product function of a Gaussian and a Lorentzian:

$$I(E) = H\exp(-B_G(E-E_0)^2)/[1+B_L(E-E_0)^2] \quad (2)$$

where $B_G$ and $B_L$ are half width parameters of a Gaussian part and a Lorentzian part, respectively. $H$ is the peak height at the peak center ($E_0$).

## Computational Method

The molecular orbital (MO) calculation of compounds such as oxyacids including transition metals by the first principles is one of the interesting problems. Discrete variational (DV) X$\alpha$ method based on the self-consistent Hartree–Fock–Slater (HFS) one-electron model with the statistical approximation of exchange-correlation has successfully been applied to many problems.[15] In the DVX$\alpha$ the matrix elements of Hamiltonian and overlap integrals are calculated as weighted sums of integrand values at discrete sample points. In the present calculation, numerical basis functions were utilized.

The exchange-correlation term is given by a statistical local expression:

$$V_{xc}(r) = -3\alpha[(3/8\pi)\rho(r)]^{1/3} \quad (3)$$

where $\alpha$ is the only parameter used in the DVX$\alpha$ method. For many metal complexes, it has been shown that theoretical dipole moments as well as ionization energies are in excellent agreement with experimental values when $\alpha$=0.7 is used.[16] Therefore, $\alpha$=0.7 was used throughout the present calculation.

In this calculation, one-electron energy is given by the partial derivative of the total energy with respect to the occupation number of orbital $i$. Here, a concept "transition state" is useful to determine excitation energies. The excitation energy from the $i$th orbital to the $j$th orbital is given as the difference of the corresponding eigenvalues $\varepsilon_j - \varepsilon_i$ for the transition state, where a half electron is removed from the $i$th orbital and put into the $j$th orbital.[15]

Evaluation of the peak intensity is possible by using the modified routine of the so-called SXS calculation developed for the study of the soft X-ray emission spectroscopy.[17] Here, the transition probability $I_{vc}$ for the transition where an electron in the initial level $v$ falls into the final level $c$ is written as

$$I_{vc} \sim E_{vc}^3 \mid \Sigma(i,j)C_{iv}C_{jc} < \phi_i \mid er \mid \phi_j > \mid^2 \quad (4)$$

where $E_{vc}$ is the transition energy between two levels $v$ and $c$; $\phi_i$ and $\phi_j$ are the numerical basis functions. The eigenvector $C_{iv}$ and $C_{jc}$ based on an LCAO scheme can be obtained from the MO calculation.

In the DV numerical integration scheme, all integrals in this equation are evaluated as weighted sums of integrand values at sample points taken in the three-dimensional real space. Rigorous calculations of this equation are possible without any approximation. When the transition state is taken for the calculation, the orbital reconstruction effects between the initial and the final state are properly included in the transition-state cluster. It means that the peak intensity calculated is more accurate with the transition-state

cluster rather than with that of the ground-state. In actual calculation, a part of Eq. 4, so called square of the transition momentum

$$|\Sigma(i,j)C_{iv}C_{jc} < \phi_i|er|\phi_j > |^2, \quad (5)$$

is calculated as an estimation of a peak intensity. In order to make easy the comparison of the observed spectrum to the reproduced one by the MO, the latter was convoluted by Eq. 2 with the half width parameters, $B_G$=16.0 and $B_L$=0, throughout this study.

On the other hand the Mulliken population analysis gives bond overlap population called bond order, which is a measure of the strength of covalency. Although the DVX$\alpha$ method is not suitable for the calculation of accurate total energy,[18] evaluation of this bond order gives a good criterion on the stability of the cluster.

The basis sets for the DVX$\alpha$ include Cr 1s-4p, O 1s-2p, and H 1s. The used computers were a Sony NWS 3860 workstation for the DVX$\alpha$, and an NEC9801 for data treatments including the FAEC.

## Results and Discussion

**Cluster Model of $CrO_4^{2-}$ Giving the Best Fit to UV-vis Spectrum.** In Fig. 2 the observed spectrum of chromate ion, $CrO_4^{2-}$, is shown at the first panel; and the result of the peak separation at the second panel. The structure of the $CrO_4^{2-}$ has been reported as tetrahedral ($T_d$); and the interatomic distances between Cr–O in crystals are about 1.60 Å for $Na_2CrO_4$.[19] 1.64 Å for $CaCrO_4$,[20] 1.60 Å for $(NH_4)_2CrO_4$.[21] A hypothetical octahedral ($O_h$) structure shown in A2 of Fig. 1 was also examined for comparison. This species A2 with six equivalent Cr–OH bonds, $Cr(OH)_6^{2-}$, can be rewritten in another way as $CrO_4^{2-}\cdot(H_2O)_2$. Furthermore, a hydrated $T_d$ species $CrO_4^{2-}\cdot(H_2O)_4$ shown in A3 of Fig. 1 was also examined.

When the Cr–O distance 1.62 Å was used for the structure A1, the molecular orbital levels were given as shown in Fig. 3. A molecular orbital level $1t_{1a}$ is the highest occupied orbital, and $2e_1$ is the lowest unoccupied orbital. The occupied orbitals are mainly consisted of 2p orbitals of oxygen atoms; and the unoccupied orbitals are mainly consisted of 3d orbitals of Cr atom. Therefore the electronic transitions are categorized to the charge-transfer transition from oxygen 2p orbital to chromium 3d orbital. The lowest energy transition corresponding to the transition from $1t_{1a}$ to $2e_1$ is 4.69 eV; however, it is too large as compared with the peak energy observed as the lowest energy absorption of the component spectrum, 3.35 eV. When the Cr–O distance was altered, the reproduced spectrum came to agree with the observed one at Cr–O=1.77 Å as shown in A1 panel of Fig. 2. This distance is about 10% long as compared with those reported for the most crystals. The ones obtained for the melten solution by using the EXAFS method are still 1.613—1.617 Å.[22]

This discrepancy seems to be coming from two causes:

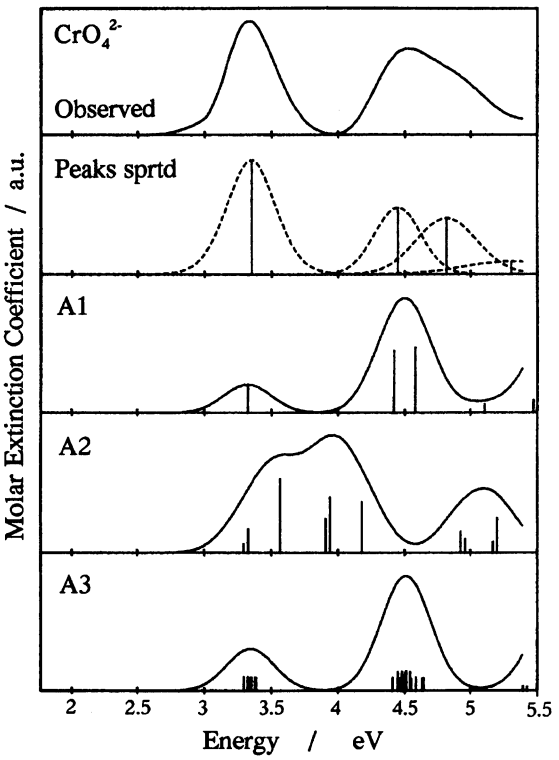


Fig. 2. First panel: component spectrum of chromate ion $CrO_4^{2-}$; the second panel: result of peak separation; and the spectra reproduced from DVX$\alpha$-MO calculation using the cluster models, A1, A2, and A3.

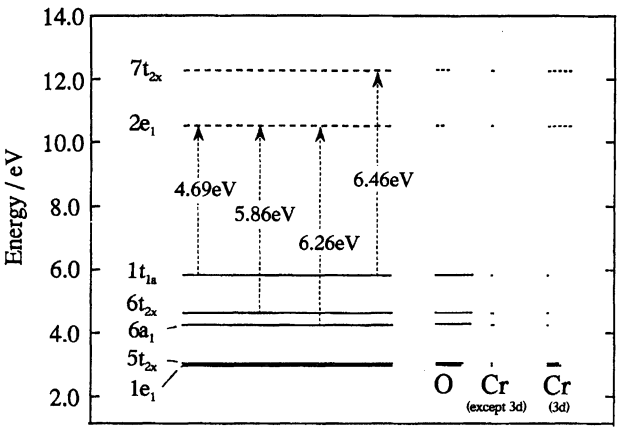


Fig. 3. Energy levels of the $CrO_4^{2-}$ species with Cr–O distance 1.62 Å for transition state cluster A1; and the contributions of atomic orbitals.

The first is that the A1 cluster of $CrO_4^{2-}$ is the one put in vacuum. In solution $CrO_4^{2-}$ ion is surrounded by some water molecules. The A3 cluster of Fig. 1 is the one that the $CrO_4^{2-}$ is assumed to be surrounded by four water molecules. In this cluster, the hydrogen bond length (Cr)O–H–O(H) was taken as 2.85 Å, according to a literature where the hydration structure of perchlorate ion was studied by X-ray diffraction method.[23] Then, the optimum Cr–O distance becomes a little bit shorter value 1.74 Å; and the reproduced spectrum is A3

of Fig. 2. It means that when the effect of hydration is rigorously taken into account, the optimum Cr–O distance becomes much shorter.

Another reason for the discrepancy in the Cr–O distances is ascribed to the uniqueness of the absorption peak observed at 3.35 eV. This absorption has been assigned to a vibronic transition, coupling with the totally symmetrical vibrational excitation. The vibration is in rigorous resonance with the electronic transition. Using the crude Franck–Condon model, a study on the excited state geometry for the $CrO_4^{2-}$ has reported that in aqueous solution the excited state Cr–O bond length may be expanded by 0.115 Å than that in the ground state.[24] Then 1.62 Å+0.115 Å becomes 1.735 Å; this value is very close to the one (1.74 Å) used at the hydrated cluster A3.

It seems that the Cr–O distance now obtained for the cluster A1, 1.77 Å, is a kind of parameter which takes into account the solvation effect and the vibronical effect under irradiation from light source of the spectrophotometer. In the following discussion, we ignored the solvating waters from cluster models, and simply adjusted the distance between Cr–O so as that the reproduced spectrum fitted to the observed spectrum.

The fitting in shape of the component spectrum to the reproduced one from MO is very good when the A1 (and A3) cluster is used. However, when an another cluster model A2 with the $O_h$ center is used, the shape of the reproduced spectrum A2 of Fig. 2 differs from the component spectrum. In this case, the distance between O–H was kept constant 0.96 Å, and the distance between Cr–O was optimized so that the lowest energy transition peak of the reproduced spectrum consisted to that of the component spectrum. It means that the $O_h$ centered cluster is not adequate to represent the real structure of the $CrO_4^{2-}$ ion in solution.

On the other hand, the bond order obtained from Mulliken's population analysis gives large positive value 0.383 to the Cr–O bonds when the A1 cluster ($T_d$) used, but some large negative value −0.370 when the A2 ($O_h$) cluster used, as shown in Table 1. The bond order is a measure of covalency. The large positive value means a strong covalent bond, and the negative value means an anti-bonding character. Negative values of the A2 cluster indicate again that the $O_h$ cluster is not favored. As a result, we can conclude that the chromate ion, $CrO_4^{2-}$, exists as the $T_d$ ion not as the $O_h$ ion, only from the interpretation of its UV-vis spectrum, although this conclusion is so well known to us.

**Cluster Model of $HCrO_4^-$ Giving the Best Fit to UV-vis Spectrum.** In Fig. 4, the observed spectrum of hydrogen chromate ion ($HCrO_4^-$), the result of the peak separation, and the spectra obtained by the MO calculations assuming B1, B3, and B4 clusters (Fig. 1) are shown. In any cluster, the distance between O–H was kept constant 0.96 Å, and Cr–O distance was optimized. Even for this ion, the discrepancy between

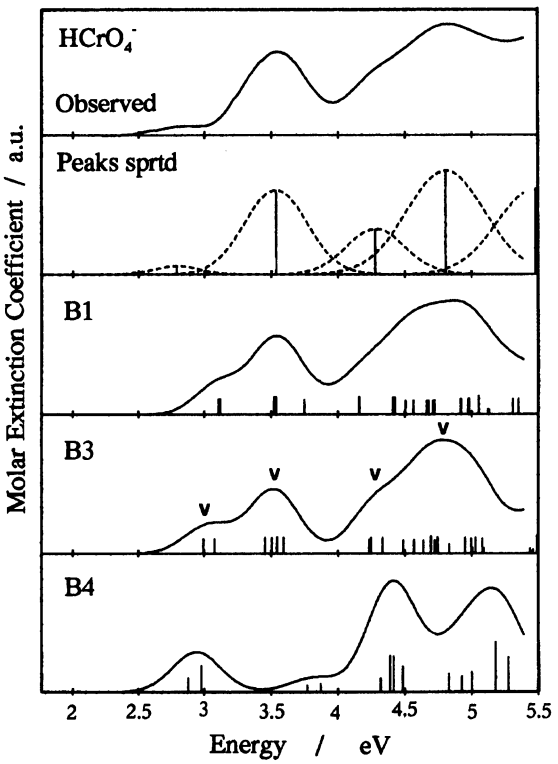


Fig. 4. First panel: component spectrum of hydrogen chromate ion $HCrO_4^-$; the second panel: result of peak separation; and the spectra reproduced from DVX$\alpha$-MO calculation using the cluster models, B1, B3, and B4. The 'v' marks denote the possible component peaks corresponding to the ones separated at the second panel.

the observed spectrum and the reproduced one assuming the $O_h$ cluster B4 was obvious. It is concluded that the $HCrO_4^-$ ion has a $T_d$ center, not an $O_h$ center. The reproduced spectrum using the cluster B2 is not shown in Fig. 4, but is almost same as that of B3 of Fig. 4. Among B1, B2, and B3 having the $T_d$ center, the B1 has a straight Cr–O–H bond. And in the B2 and the B3, the Cr–O–H bond is bent; the angle of Cr–O–H has been assumed to be 109° 28′, the ideal tetrahedral angle. In the B2 case, the hydrogen atom is existing just over another Cr–O bond; but in the B3 case, the hydrogen atom is existing over the mid of other two Cr–O bonds. The reproduction by the MO gave the closest spectrum at the B3 (or the B2) cluster to the component spectrum. The 'v' marks in the B3 panel of Fig. 4 denote possible component peaks corresponding to the ones separated at the second panel of Fig. 4. The Cr–O bond orders also took the maximum values (0.406 and 0.046) when the B3 cluster was used. When the B2 cluster was used, the bond orders became a little bit smaller. Thus, the B3 cluster seems to be the most preferable structure of the $HCrO_4^-$ ion, although the B2 and the B3 seem to be easily altered as the hydrogen atom can rotate around an upward Cr–O bond.

**Cluster Model of $H_2CrO_4$ Giving the Best Fit**

Table 1. The Values of Bond Length and Bond Angle

| Structure[b] | Interatomic distance/Å | | | Net charge | | | | Bond order | | |
|---|---|---|---|---|---|---|---|---|---|---|
| | Cr–$O_t$ | Cr–$O_b$ | O–H | Cr | $O_t$[a] | $O_b$[a] | H | Cr–$O_t$ | Cr–$O_b$ | $O_b$–H |
| $CrO_4^{2-}$ | | | | | | | | | | |
| A1 | 1.77 | | | +1.962 | −0.991 | | | 0.383 | | |
| A2 | 1.60 | 1.60 | 0.96 | +3.313 | −1.082 | −1.290 | +0.502 | 0.101 | −0.370 | 0.535 |
| $HCrO_4^-$ | | | | | | | | | | |
| B1 | 1.73 | 1.73 | 0.96 | +2.099 | −0.813 | −1.181 | +0.521 | 0.399 | 0.007 | 0.545 |
| B2 | 1.73 | 1.73 | 0.96 | +2.034 | −0.810 | −1.078 | +0.474 | 0.401 | 0.025 | 0.514 |
| B3 | 1.73 | 1.73 | 0.96 | +2.020 | −0.808 | −1.069 | +0.472 | 0.046 | 0.046 | 0.516 |
| B4 | 1.65 | 1.65 | 0.96 | +3.139 | −0.776 | −1.187 | +0.514 | 0.297 | −0.129 | 0.539 |
| $H_2CrO_4$ | | | | | | | | | | |
| C1 | 1.73 | 1.73 | 0.96 | +2.183 | −0.583 | −1.088 | +0.580 | 0.465 | 0.102 | 0.522 |
| C2 | 1.73 | 1.73 | 0.96 | +2.009 | −0.578 | −0.940 | +0.513 | 0.484 | 0.148 | 0.504 |
| C3 | 1.73 | 1.73 | 0.96 | +2.014 | −0.600 | −0.917 | +0.510 | 0.484 | 0.148 | 0.506 |
| C4 | 1.68 | 1.68 | 0.96 | +3.151 | | −1.089 | +0.564 | | −0.007 | 0.522 |
| $Cr_2O_7^{2-}$ | | | | | | | | | | |
| D | 1.72 | 1.85 | | +1.961 | −0.815 | −1.031 | | 0.428 | 0.214 | |

a) $O_t$ : terminal oxygen; $O_b$ : bridging oxygen such as Cr–O–H, Cr–O–Cr. b) bond angle ∠O–Cr–O 109° 28′ (A1, B1, B2, B3, C1, C2, C3, D); 90° (A2, B4, C4). bond angle ∠Cr–$O_b$–Cr 120° (D).

**to UV-vis Spectrum.** In Fig. 5, the observed spectrum of dihydrogen chromate ($H_2CrO_4$), the result of peak separation, and the spectra obtained by the MO calculation assuming C1, C2, C3, and C4 clusters of Fig. 1 are shown. In any cluster, the distance between the O–H was kept constant 0.96 Å, and the Cr–O distance was optimized. In this case, the possible orientations of bonds are so flexible that the fitness of the component spectrum to the reproduced one is not better as compared with the case of the $CrO_4^{2-}$ or the $HCrO_4^-$. However, it is obvious that the discrepancy between the observed spectrum and the one reproduced assuming the $O_h$ center C4 is large. The $H_2CrO_4$ has not an $O_h$ center. The clusters C1, C2, and C3 have the $T_d$ center. The cluster model C1 has two straight Cr–O–H bonds. On the other hand, there a lot of combinations of bending forms of Cr–O–H bond, such as C2 and C3. Thirteen typical combinations were examined. As a result, the cluster C2 seemed to be the most preferable one when the result of peak separation and the peak positions of the C2 cluster (denoted by the 'v' marks) were examined. In addition, this cluster C2 has the largest bond orders of the Cr–O (0.484 and 0.148) among the candidates. Thus, the C2 cluster is favored, but is not necessarily only possible cluster in solution because two hydrogen atoms can rotate around their connecting Cr–O bonds.

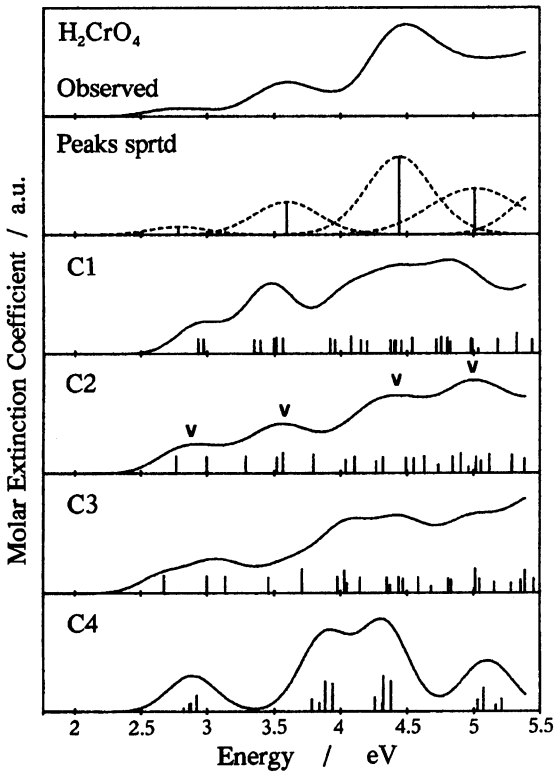


Fig. 5. First panel: component spectrum of dihydrogen chromate $H_2CrO_4$; the second panel: result of peak separation; and the spectra reproduced from DVX$\alpha$-MO calculation using the cluster models, C1, C2, C3, and C4. The 'v' marks denote the possible component peaks corresponding to the ones separated at the second panel.

**Cluster Model of $Cr_2O_7^{2-}$ Giving the Best Fit to UV-vis Spectrum.** In Fig. 6, the observed spectrum of dichromate ion ($Cr_2O_7^{2-}$), the result of peak separation, and the spectrum obtained by the MO calculation assuming the cluster D are shown. In this case, the distance between the O–H was kept constant 0.96

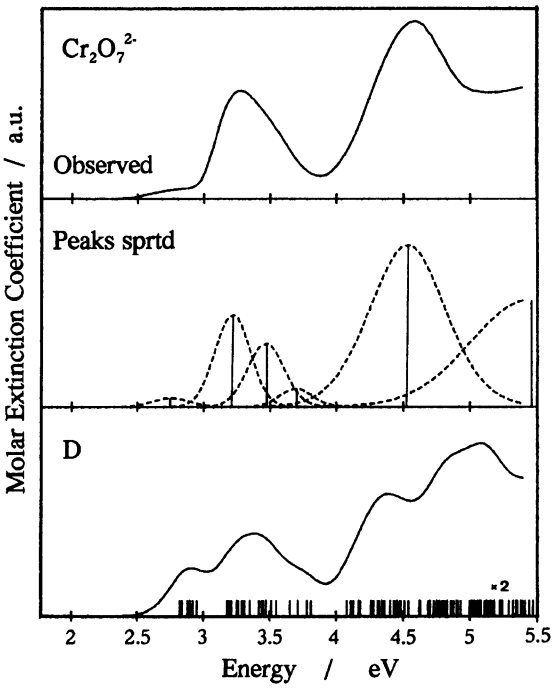


Fig. 6. First panel: component spectrum of dichromate ion $Cr_2O_7^{2-}$; the second panel: result of peak separation; and the spectra reproduced from DVX$\alpha$-MO calculation using the cluster model D.

Å, and two kinds of Cr–O distances — one is Cr–$O_t$ (terminal), and the other is Cr–$O_b$ (bridge) — were optimized. In this estimation of peak intensities (Eq. 5), the calculation did not converge; thus all peak intensities were set to be same in order to reproduce the component spectrum. As a result, the D cluster shown in Fig. 1 was recommended, which gave the best fit between the observed spectrum and the one reproduced from MO calculation. This cluster gave the large positive values (0.428 and 0.214) to the bond orders.

**Interpretation of Dimerization Reaction Based on Bond Orders.** In the above discussion, two kinds of criteria were used to assign the preferable structure to each species: The first is the degree of fitness between the observed component spectrum with the one reproduced from the MO. The second is the value of the bond orders among pairs of atoms constructing the cluster. The bond order is a measure of the covalency. The bigger the bond order, the stronger the covalency, and more stable the species is. Table 1 shows that the bond order of Cr–OH of the $HCrO_4^-$, 0.046, is smaller by almost one order than that of Cr–O of the $CrO_4^{2-}$, 0.383, and than that of Cr–OH of the $H_2CrO_4$, 0.148.

We have recognized that the quantity, bond order, can be used to understand the lability of a reaction. Now consider the dimerization reaction shown by Eq. 1. The equilibrium constant $K_D$ can be expressed by using a rate constant of the forward reaction $k_+$ and that of the backward reaction $k_-$ :

$$K_D = k_+/k_- \tag{6}$$

If an activated state complex expressed as B of Fig. 7 is assumed, and if it is allowed to assume that the bond orders of the dotted bonds of this complex (B) are sufficiently small, the forward rate constant $k_+$ (for dimerization: A→B) should be proportional to the easiness of the break of $O_3$Cr–OH bond (a1) and that of $O_3$CrO–H (a2). On the other hand, the backward rate constant $k_-$ (for monomerization: C→B) should be proportional to the easiness of the break of $O_3$Cr–O$CrO_3$ (c1) and that of HO–H (c2). From the Table 1, the bond order of Cr–O in the $O_3$Cr–O$CrO_3$ (c1: 0.214) is larger than that in the $O_3$Cr–OH (a1: 0.046); and the bond order of O–H in the HO–H (c2: 0.523) is larger than that in the $O_3$CrO–H (a2: 0.516). Here, the bond order HO–H in $(H_2O)_5$ cluster was otherwise calculated. These comparison of bond orders indicate that the $k_-$ is smaller than the $k_+$; in another word, the dimerization is much favored as compared with the monomerization. In fact, the rate constants for a following reaction have been reported:[25]

$$H^+ + HCrO_4^- + HCrO_4^- \underset{k_-}{\overset{k_+}{\rightleftharpoons}} Cr_2O_7^{2-} + H_2O + H^+ \tag{7}$$

where $k_+ = 6.2\times10^5$ $dm^6\,mol^{-2}\,s^{-1}$ and $k_- = 6.3\times10^3$ $dm^3\,mol^{-1}\,s^{-1}$. If there are sufficient number of $HCrO_4^-$ ions in solution, the formation of $Cr_2O_7^{2-}$ should

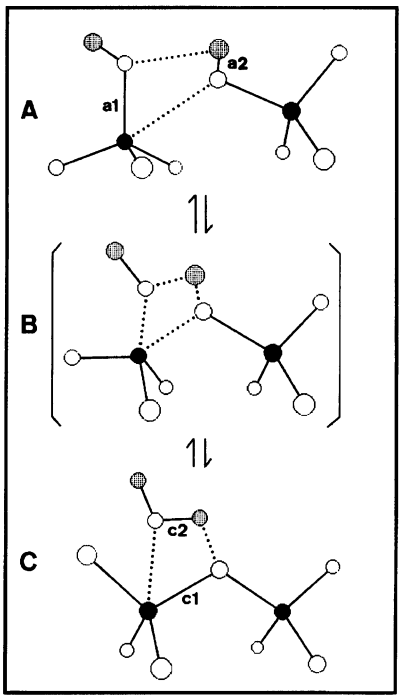


Fig. 7. Schematic illustration of dimerization/monomerization reactions; A: $HCrO_4^- + HCrO_4^-$; B: a hypothetical activated state complex; and C: $Cr_2O_7^{2-} + H_2O$. Dotted lines indicate weak interactions; and the marks a1, a2, c1, and c2 denote the bonds (See text).

be easy.

In a similar manner, a hypothetical dimerization reaction of the $H_2CrO_4$ to form a corresponding dimer species $H_2Cr_2O_7$ can be examined.

$$2H_2CrO_4 \rightleftharpoons H_2Cr_2O_7 + H_2O \quad (8)$$

If it is allowed to assume that the bond orders of the hypothetical $H_2Cr_2O_7$ are of same order with those of $Cr_2O_7^{2-}$, it comes that the bond order of Cr–O in the $(HO)O_2\underline{Cr–O}H$ ($H_2CrO_4$: 0.148) is of same order with the value of the Cr–O in the $(HO)O_2\underline{Cr–O}CrO_2(OH)$ ($H_2Cr_2O_7$: 0.214 from $Cr_2O_7^{2-}$). It means that the break of the Cr–O in the $H_2CrO_4$ is not so easy as compared with that in $HCrO_4^-$; no large enthalpic merit can be expected for the dimerization of $H_2CrO_4$ to form $H_2Cr_2O_7$. Rather, a disadvantage coming from the loss of randomness (entropic disadvantage) due to the decrease of the number of free species is expected. No confirmed report on the existence of the species $H_2Cr_2O_7$ may be reasonable from this point of view.

## Conclusion

The treatment introduced here gave the information on the dissolved structure of the species in solution only using the UV-vis absorption spectrum. In addition, once the dissolved states of the ions are known, their electronic states are estimated. This information on electronic state, especially, bond order, gives us useful information on reaction lability.

## References

1) J. K. Beattie and G. P. Haight, Jr., *Prog. Inorg. Chem.*, **17**, 93 (1972).
2) G. Schwarzenbach and J. Meier, *J. Inorg. Nucl. Cem.*, **8**, 302 (1958).
3) J. Y. Tong and E. L. King, *J. Am. Chem. Soc.*, **75**, 6180 (1953).
4) G. P. Haight, Jr., D. C. Richardson, and N. H. Colburn, *Inorg. Chem.*, **3**, 1777 (1964).
5) J. Y. Tong, *Inorg. Chem.*, **3**, 1804 (1964).
6) H. Taube and G. Gordon, *Inorg. Chem.*, **1**, 69 (1962).
7) J. D. Neuss and W. Rieman, III, *J. Am. Chem. Soc.*, **56**, 2238 (1934).
8) W. G. Davies and J. E. Prue, *Trans. Faraday Soc.*, **51**, 1045 (1955).
9) R. K. Tandon, P. T. Crisp, J. Ellis, and R. S. Baker, *Talanta*, **31**, 227 (1984).
10) T. Shen-Yang and L. Ke-An, *Talanta*, **33**, 775 (1986).
11) T. Ozeki, H. Kihara, and H. Hikime, *Anal. Chem.*, **59**, 945 (1987).
12) T. Ozeki, H.Kihara, and S. Ikeda, *Anal. Chem.*, **60**, 2055 (1988).
13) T. Ozeki, H. Adachi, and S. Ikeda, *Anal. Sci.*, **7**, 713 (1991).
14) D. Dobos, "Electrochemical Data," Elsevier Sci. Pub., Amsterdam (1975).
15) H. Adachi, M. Tsukada, and C. Satoko, *J. Phys. Soc. Jpn.*, **45**, 875 (1978).
16) E. J. Baerends and P. Ros, *Chem. Phys.*, **2**, 52 (1973).
17) H. Adachi and K. Taniguchi, *J. Phys. Soc. Jpn.*, **49**, 1944 (1980).
18) M. Sano, H. Adachi, and H. Yamatera, *Bull. Chem. Soc. Jpn.*, **54**, 2898 (1981).
19) J. J. Miller, *Z. Kristallogr.*, **94A**, 131 (1936).
20) J. H. Clouse, *Z. Kristallogr.*, **83**, 161 (1932).
21) D. I. Bujor, *Z. Kristallogr.*, **105A**, 364 (1944).
22) M. Miyake, N. Nakagawa, H. Ohyanagi, and T. Suzuki, *Inorg. Chem.*, **25**, 700 (1986).
23) K. Michelsen, *Acta Chem. Scand.*, **6**, 1289 (1952).
24) E. Campani, F. Ferri, G. Gorini, E. Polacco, and G. Masetti, *Chem. Phys. Lett.*, **107**, 91 (1984).
25) J. R. Pladziewicz and J. H. Espensen, *Inorg. Chem.*, **10**, 634 (1971).